The American Journal of Pathology, Vol. 172, No. 6, June 2008

DOI: 10.2353/ajpath.2008.071049

Immunopathology and Infectious Disease

CD19 Regulates Skin and Lung Fibrosis via Toll-Like Receptor Signaling in a Model of Bleomycin-Induced Scleroderma

Ayumi Yoshizaki,* Yohei Iwata,* Kazuhiro Komura,* Fumihide Ogawa,* Toshihide Hara,* Eiji Muroi,* Motoi Takenaka,* Kazuhiro Shimizu,* Minoru Hasegawa,† Manabu Fujimoto,† Thomas F. Tedder,‡ and Shinichi Sato*

From the Department of Dermatology, Nagasaki University Graduate School of Biomedical Sciences, Nagasaki, Japan; the Department of Dermatology,† Kanazawa University Graduate School of Medical Science, Kanazawa, Japan; and the Department of Immunology,‡ Duke University Medical Center, Durham, North Carolina*

Mice subcutaneously injected with bleomycin, in an experimental model of human systemic sclerosis, develop cutaneous and lung fibrosis with autoantibody production. CD19 is a general "rheostat" that defines signaling thresholds critical for humoral immune responses, autoimmunity, and cytokine production. To determine the role of CD19 in the bleomycin-induced systemic sclerosis model, we investigated the development of fibrosis and autoimmunity in CD19-deficient mice. Bleomycin-treated wild-type mice exhibited dermal and lung fibrosis, hyper-γ-globulinemia, autoantibody production, and enhanced serum and skin expression of various cytokines, including fibrogenic interleukin-4, interleukin-6, and transforming growth factor-β1, all of which were inhibited by CD19 deficiency. Bleomycin treatment enhanced hyaluronan production in the skin, lung, and sera. Addition of hyaluronan, an endogenous ligand for Toll-like receptor (TLR) 2 and TLR4, stimulated B cells to produce various cytokines, primarily through TLR4; CD19 deficiency suppressed this stimulation. These results suggest that bleomycin induces fibrosis by enhancing hyaluronan production, which activates B cells to produce fibrogenic cytokines mainly via TLR4 and induce autoantibody production, and that CD19 deficiency suppresses fibrosis and autoantibody production by inhibiting TLR4 signals. ***(Am J Pathol 2008, 172:1650–1663; DOI: 10.2353/ajpath.2008.071049)***

Systemic sclerosis (SSc) is a connective tissue disease characterized by excessive extracellular matrix deposition in the skin and other visceral organs with an autoimmune background.[1] The presence of autoantibodies is a central feature of SSc, because antinuclear antibodies (Abs) are detected in >90% of patients.[2] SSc patients have autoantibodies that react to various intracellular components, such as DNA topoisomerase I (topo I), centromeric protein B (CENP B), U1-ribonucleoprotein (RNP), and histones.[2] Furthermore, abnormal activation of immune cells, including T lymphocytes, B lymphocytes, natural killer cells, and macrophages, has been identified in SSc.[3–5] A recent study has shown that skin and lung fibrosis is ameliorated by treatment with cyclophosphamide, an immunosuppressive agent, indicating that immune activation leads to fibrosis through the stimulation of collagen production by fibroblasts.[6] Indeed, SSc patients exhibit elevated serum levels of various cytokines, especially fibrogenic Th2 cytokines, such as interleukin (IL)-4, IL-6, IL-10, some Th1 cytokines, such as IL-2, tumor necrosis factor (TNF)-α, and IL-12, a transforming growth factor (TGF)-β1, a major fibrogenic growth factor.

B-cell signaling thresholds are regulated by response regulators that augment or diminish B-cell signals during responses to self and foreign antigens.[7] Abnormal regulation of the response regulator function and expression may result in autoantibody production. Among these response regulators, CD19, which is a critical cell-surface signal transduction molecule of B cells, is a most potent positive regulator.[7] Transgenic mice that overexpress CD19 by approximately threefold lose tolerance and generate autoantibodies spontaneously.[8,9] Human SSc patients exhibit a 20% increase in CD19 expression, which is associated with −499G>T allele in the CD19 promoter.[10,11] This CD19 overexpression may be related to autoantibody production and hyper-γ-globulinemia in hu-

Supported by the Takeda Science Foundation (to S.S.) and the National Institutes of Health (grants CA96547, CA105001, and AI56363 to T.F.T.).

Accepted for publication March 4, 2008.

Address reprint requests to Dr. Shinichi Sato, Department of Dermatology, Nagasaki University Graduate School of Biomedical Sciences, 1-7-1 Sakamoto, Nagasaki, 852-8501, Japan. E-mail: s-sato@nagasaki-u.ac.jp.

man SSc, because mice that overexpress CD19 to a similar extent as human SSc have hyper-γ-globulinemia and elevated levels of various autoantibodies, including SSc-specific anti-topo I Ab.[12] Furthermore, SSc patients have intrinsic B-cell abnormalities characterized by chronic hyperreactivity of memory B cells.[3] In addition, the production of B-cell-activating factor belonging to the tumor necrosis factor family (BAFF), a potent B-cell stimulatory molecule, is up-regulated with an enhanced ability of SSc B cells to produce IgG and IL-6 by BAFF stimulation.[13] Thus, intrinsic B-cell abnormalities may play a role in the systemic autoimmunity of SSc.

The loss of CD19 expression in a tight-skin (TSK) mouse, a genetic, spontaneous model of SSc, results in the inhibition of chronic B-cell hyperreactivity and in the elimination of autoantibody production, which is associated with improvement of skin fibrosis and a parallel decrease in IL-6 production by B cells.[14] Furthermore, B-cell depletion by anti-CD20 Ab or treatment with BAFF antagonists improves skin fibrosis in TSK mice.[15,16] These findings suggest that B cells play a critical role in the development of fibrosis as well as autoantibody production in TSK mice. However, this hypothesis has not been proven, because there are important differences in SSc between the TSK mouse model and humans. First, skin fibrosis in TSK mice occurs in the subcutaneous loose connective tissue layer, which does not exist in humans; in contrast, fibrosis in human SSc occurs in the dermis. Second, inflammation of the dermis, which regulates skin fibrosis by producing cytokines in human SSc, is very modest in TSK mice. Third, TSK mice exhibit lung emphysema, whereas human SSc is associated with lung fibrosis. Finally, because SSc occurs in only 1.6% of families with SSc,[17] human SSc is not a genetic disorder as it is in TSK mice. Recently, Yamamoto and colleagues[18,19] established a new mouse model of SSc using bleomycin (BLM) treatment: the subcutaneous injection of BLM induces fibrosis in the dermis and lung, autoantibody production, and dermal inflammatory infiltration, which more closely mimics the features of human SSc than that of TSK mice. However, the contribution of B cells and CD19 to disease manifestations and autoimmunity, and the mechanisms underlying B-cell activation by BLM, remain unknown in the BLM-induced SSc model. In this study, we investigated the role of CD19 in the development of autoimmunity and fibrosis induced by BLM using CD19-deficient ($CD19^{-/-}$) mice. The results of this study indicate that CD19 regulates fibrogenic cytokine production by B cells mainly through Toll-like receptor (TLR) 4 signaling, which was activated by hyaluronan, an endogenous TLR4 ligand that is up-regulated in the dermis and lung by BLM treatment: CD19 thus controls skin and lung fibrosis, hyper-γ-globulinemia, and autoantibody production induced by BLM treatment.

Materials and Methods

Mice

$CD19^{-/-}$ (C57BL/6 × 129) mice were generated as described[20] and backcrossed 7 to 12 generations onto the C57BL/6 background before use in this study. Lack of cell surface CD19 expression was verified by two-color immunofluorescence staining with flow cytometric analysis. All mice were housed in a specific pathogen-free barrier facility and screened regularly for pathogens. The mice used in these experiments were 6 weeks of age. All studies and procedures were approved by the Committee on Animal Experimentation of Nagasaki University Graduate School of Medical Science.

BLM Treatment

BLM (Nippon Kayaku, Tokyo, Japan) was dissolved in phosphate-buffered saline (PBS) at a concentration of 1 mg/ml and sterilized by filtration. BLM or PBS (300 μg) was injected subcutaneously into the shaved backs of the mice daily for 4 weeks with a 27-gauge needle, as described previously.[18]

Histopathological Assessment of Dermal Fibrosis

Morphological characteristics of skin sections were compared between $CD19^{-/-}$ and wild-type (WT) mice treated with either BLM or PBS under a light microscope. All skin sections were taken from the para-midline, lower back region (the same anatomical site, to minimize regional variations in thickness) as full-thickness sections extending down to the body wall musculature. Tissues were fixed in 10% formaldehyde solution for 24 hours and embedded in paraffin. Sections were stained with hematoxylin and eosin (H&E). Dermal thickness, defined as the thickness of skin from the top of the granular layer to the junction between the dermis and subcutaneous fat, was examined. Ten random measurements were taken per section. All of the sections were examined independently by two investigators in a blinded manner. The skin from male mice was generally thicker than that from female mice despite the BLM or PBS treatment (data not shown). Because similar results were obtained when male or female mice were analyzed separately, only data from female mice were presented for skin thickness in this study. Mast cells were identified by toluidine blue staining. Cells containing metachromatic granules were counted in 10 random grids under high-magnification (×400) power fields of a light microscope.

Immunohistochemical Staining

Frozen tissue sections of skin biopsies were acetone-fixed and then incubated with 10% normal rabbit serum in PBS (10 minutes, 37°C) to block nonspecific staining. Sections were then incubated with rat monoclonal Ab (mAb) specific for macrophages (F4/80; Serotec, Oxford, UK), B220 (BD PharMingen, San Diego, CA), CD4 (clone RM4-5, BD PharMingen), and CD8 (clone 53-6.7, BD PharMingen). Rat IgG (Southern Biotechnology Associates, Birmingham, AL) was used as a control for nonspecific staining. Sections were then incubated sequentially

(20 minutes, 37°C) with a biotinylated rabbit anti-rat IgG (Vectastain ABC kit; Vector Laboratories, Burlingame, CA) and horseradish peroxidase-conjugated avidin-biotin complexes (Vectastain ABC kit, Vector Laboratories). Sections were developed with 3,3′-diaminobenzidine tetrahydrochloride and hydrogen peroxide, and then counterstained with methyl green. Stained cells were counted in 10 random grids under high-magnification (×400) power fields of a light microscope. Each section was examined independently by two investigators in a blinded manner.

Histopathological Assessment of Lung Fibrosis

Lungs were excised after 4 weeks of treatment with BLM or PBS, processed as previously described,[21] and stained by H&E and van Gieson to detect collagen. The severity of fibrosis was semiquantitatively assessed according to Ashcroft and colleagues.[21] Briefly, the lung fibrosis was graded on a scale of 0 to 8 by examining randomly chosen fields of the left middle lobe at a magnification of ×100. The grading criteria were as follows: grade 0, normal lung; grade 1, minimal fibrous thickening of alveolar or bronchiolar walls; grade 3, moderate thickening of walls without obvious damage to lung architecture; grade 5, increased fibrosis with definite damage to lung structure and formation of fibrous bands or small fibrous masses; grade 7, severe distortion of structure and large fibrous areas; and grade 8, total fibrous obliteration of fields. Grades 2, 4, and 6 were used as intermediate pictures between the aforementioned criteria. All of the sections were scored independently by two investigators in a blinded manner.

Hyaluronan Staining

Formalin-fixed and paraffin-embedded tissues were cut into sections of 4 μm in thickness, deparaffinized in xylene, and rehydrated in PBS. Deparaffinized sections were preincubated with 1% H_2O_2 for 5 minutes to block tissue peroxidase activity. The sections were then incubated with bovine serum albumin in PBS for 30 minutes at 37°C, followed by overnight incubation at 4°C with 3 mg/ml of biotinylated hyaluronic acid-binding protein (Sigma-Aldrich, St. Louis, MO). After washing with PBS, the slides were incubated with streptavidin-horseradish peroxidase (BD PharMingen) for 1 hour, and the reaction products were visualized using diaminobenzidine with methyl green as counterstaining. The specificity of the staining was confirmed by preincubating the sections with *Streptomyces*-derived hyaluronidase to remove hyaluronan from the tissue.

Enzyme-Linked Immunosorbent Assay (ELISA) for Serum Cytokines and Hyaluronan

Sera were obtained by a cardiac puncture after 4 weeks of treatment with BLM or PBS and were stored at −80°C. Serum levels of IL-4, IL-6, IL-10, interferon (IFN)-γ, TGF-β1, TNF-α, and macrophage inflammatory protein (MIP)-2 were assessed using specific ELISA kits (IL-4, IL-6, IL-10, IFN-γ, TGF-β1, and TNF-α: Biosource International, Camarillo, CA; and MIP-2: Peprotech, London, UK). The amount of hyaluronan in the serum was quantified using an ELISA kit (Echelon Biosciences, Salt Lake City, UT).

Antinuclear Ab Analysis

Antinuclear Abs were assessed by indirect immunofluorescence staining using sera diluted 1:50 and HEp-2 substrate cells (Medical & Biological Laboratories, Nagoya, Japan) as described.[10] Antinuclear Abs were detected using fluorescein isothiocyanate-conjugated $F(ab')_2$ fragments specific for mouse IgG + IgM + IgA (Southern Biotechnology Associates).

ELISAs for Autoantibodies

The specific ELISA kits were used to measure anti-topo I (Medical & Biological Laboratories), anti-CENP B (Funakoshi, Tokyo, Japan), anti-U1-RNP (Medical & Biological Laboratories), anti-histone (Funakoshi), anti-single-stranded DNA (ssDNA; Shibayagi, Gunma, Japan), and anti-double-stranded DNA (dsDNA; Medical & Biological Laboratories) Ab and rheumatoid factor (Shibayagi). These ELISA plates were incubated with serum samples diluted 1:100. Relative levels of autoantibodies were determined for each group of mice using pooled serum samples. Sera were diluted at log intervals (1:10 to $1:10^5$) and assessed for relative autoantibody levels as above except that the results were plotted as OD versus dilution (log scale). The dilutions of sera giving half-maximal OD values were determined by linear regression analysis, thus generating arbitrary units per ml values for comparison between sets of sera.

Mouse Ig Isotype-Specific ELISA

To determine Ab concentrations in sera, ELISA was performed as described,[20] using affinity-purified mouse IgM, IgG1, IgG2a, IgG2b, IgG3, and IgA (Southern Biotechnology Associates) to generate standard curves. The relative Ig concentration of each sample was calculated by comparing the mean OD obtained for duplicate wells to a semilog standard curve of titrated standard Ab using linear regression analysis.

RNA Isolation and Real-Time Polymerase Chain Reaction (PCR)

Total RNA was isolated from lower back skin with RNeasy spin columns (Qiagen, Crawley, UK). Total RNA from each sample was reverse-transcribed into cDNA. Expression of IL-4, IL-6, IL-10, IFN-γ, TGF-β1, TNF-α, and MIP-2 was analyzed using a real-time PCR quantification method according to the manufacturer's instructions (Applied Biosystems, Foster City, CA). Sequence-specific

primers and probes were designed by Pre-Developed TaqMan assay reagents or Assay-On-Demand (Applied Biosystems). Real-time PCR (40 cycles of denaturing at 92°C for 15 seconds and annealing at 60°C for 60 seconds) was performed on an ABI Prism 7000 sequence detector (Applied Biosystems). Glyceraldehyde-3-phosphate was used to normalize mRNA. Relative expression of real-time PCR products was determined by using the ΔΔCt method[22] to compare target gene and housekeeping gene mRNA expression. One of the control samples was chosen as a calibrator sample.

B-Cell Purification and Stimulation

Splenic B cells were purified (>95% $B220^+$) by removing T cells with anti-Thy1.2 Ab-coated magnetic beads (Dynal, Lake Success, NY), and subsequently lysed in buffer containing 1% Nonidet P-40 as described.[23] The purified splenic B cells were stimulated in 0.6 ml of culture medium in 48-well flat-bottom plates with 25, 50, or 100 ng/ml of BLM in the presence of 1 μg/ml of lipopolysaccharide (LPS, Sigma-Aldrich). In other experiments, B cells were stimulated with 200 μg/ml of hyaluronan that contained both high- and low-molecular weight hyaluronan (50 to 8000 kDa; Biomedicals, Irvine, CA), 200 μg/ml only low-molecular weight hyaluronan (15 to 40 kDa; R&D Systems, Minneapolis, MN), 100 μg/ml heparan sulfate (Biomedicals), 200 μg/ml chondroitin sulfate (Biomedicals), or 500 ng/ml high-mobility group box 1 protein (HMGB-1, Sigma-Aldrich) for 10 hours. Anti-mouse TLR4 mAb (Imgenex, San Diego, CA) or control rat IgG2a (R&D Systems) was added 60 minutes before hyaluronan stimulation at concentrations of 100 μg/ml. Expression of IL-4, IL-6, IL-10, IFN-γ, TGF-β1, TNF-α, and MIP-2 was analyzed using a real-time PCR quantification method. Culture supernatants from unstimulated or stimulated B cells were also analyzed for the production of these cytokines by specific ELISA kits.

Statistical Analysis

All data are expressed as mean values ± SD. The Mann-Whitney *U*-test was used to determine the level of significance of differences between sample means, and Bonferroni's test was used for multiple comparisons.

Results

CD19 Loss Attenuated the Development of Skin and Lung Fibrosis Induced by BLM

BLM was injected subcutaneously into the backs of mice daily for 4 weeks. Previous studies have shown that skin fibrosis, lung fibrosis, epithelial injury, and inflammatory cell infiltration develop during the first 4 weeks of BLM treatment, peak in the 4th week, and begin to resolve 6 weeks after the cessation of treatment.[18,24–27] In this study, skin and lung fibrosis in $CD19^{-/-}$ and WT mice treated with either BLM or PBS was histopathologically assessed 1, 2, 3, and 4 weeks after the initiation of BLM treatment. Dermal thickness and lung fibrosis score showed time-dependent increases in BLM-treated mice (Figure 1, a and d). After 2 weeks of treatment, BLM treatment induced significantly greater dermal thickness relative to PBS treatment in WT mice ($P < 0.05$) but not in $CD19^{-/-}$ mice, although there was no significant difference in the dermal thickness between WT and $CD19^{-/-}$ mice at this time point. After 3 weeks, a significant difference in the dermal thickness between WT and $CD19^{-/-}$ mice was apparent ($P < 0.005$). After 4 weeks, the dermal thickness in BLM-treated WT mice significantly increased by 1.9-fold compared with PBS-treated WT mice ($P < 0.005$; Figure 1, a–c). In contrast, BLM-treated $CD19^{-/-}$ mice showed moderate thickening of dermal tissue that was significantly 27% thinner than that found in BLM-treated WT mice ($P < 0.005$), but remained thicker than that of PBS-treated $CD19^{-/-}$ and WT mice ($P < 0.005$). Masson trichrome staining revealed thickened collagen bundles in the skin from BLM-treated WT mice, which was also reduced by CD19 deficiency (data not shown). Similar results were obtained for the lung fibrosis score, except that a significant difference in the lung fibrosis score between WT and $CD19^{-/-}$ mice was detected after 2 weeks (Figure 1d). After 4 weeks of BLM administration, BLM-treated WT mice exhibited extensive inflammatory infiltration, fibrosis, granulomas, and alveolar epithelial injury (Figure 1, e and f). In contrast, CD19 deficiency reduced such histological changes. Thus, subcutaneous BLM injection induced skin and lung fibrosis that CD19 deficiency attenuated.

CD19 Loss Inhibited Dermal Inflammatory Infiltration

The numbers of mast cells, macrophages, T cells, and B cells have been reported to increase in sclerotic skin from human SSc.[5,25,28,29] Therefore, we counted these immune cells at the BLM-injected sites. Among WT mice, the numbers of mast cells, macrophages, T cells, and B cells were greater in BLM-treated WT mice than in PBS-treated WT mice ($P < 0.005$; Figure 2, a–d, respectively). BLM-treated $CD19^{-/-}$ mice showed lower infiltration of these cells than BLM-treated WT mice ($P < 0.005$), but still greater infiltration than PBS-treated $CD19^{-/-}$ mice ($P < 0.005$).

CD19 Deficiency Suppressed BLM-Induced Overproduction of Cytokines in the Skin and Serum

It has been suggested that IL-4, IL-6, IL-10, IFN-γ, TNF-α, and TGF-β1 production contributes to BLM-induced fibrosis by regulating the production of collagen and glycosaminoglycans by fibroblasts.[18,19,30–32] Furthermore, MIP-2, one of the murine IL-8 homologues, may be a potential candidate for explaining the reduction of mast cells, macrophages, and T cells in the fibrotic skin from

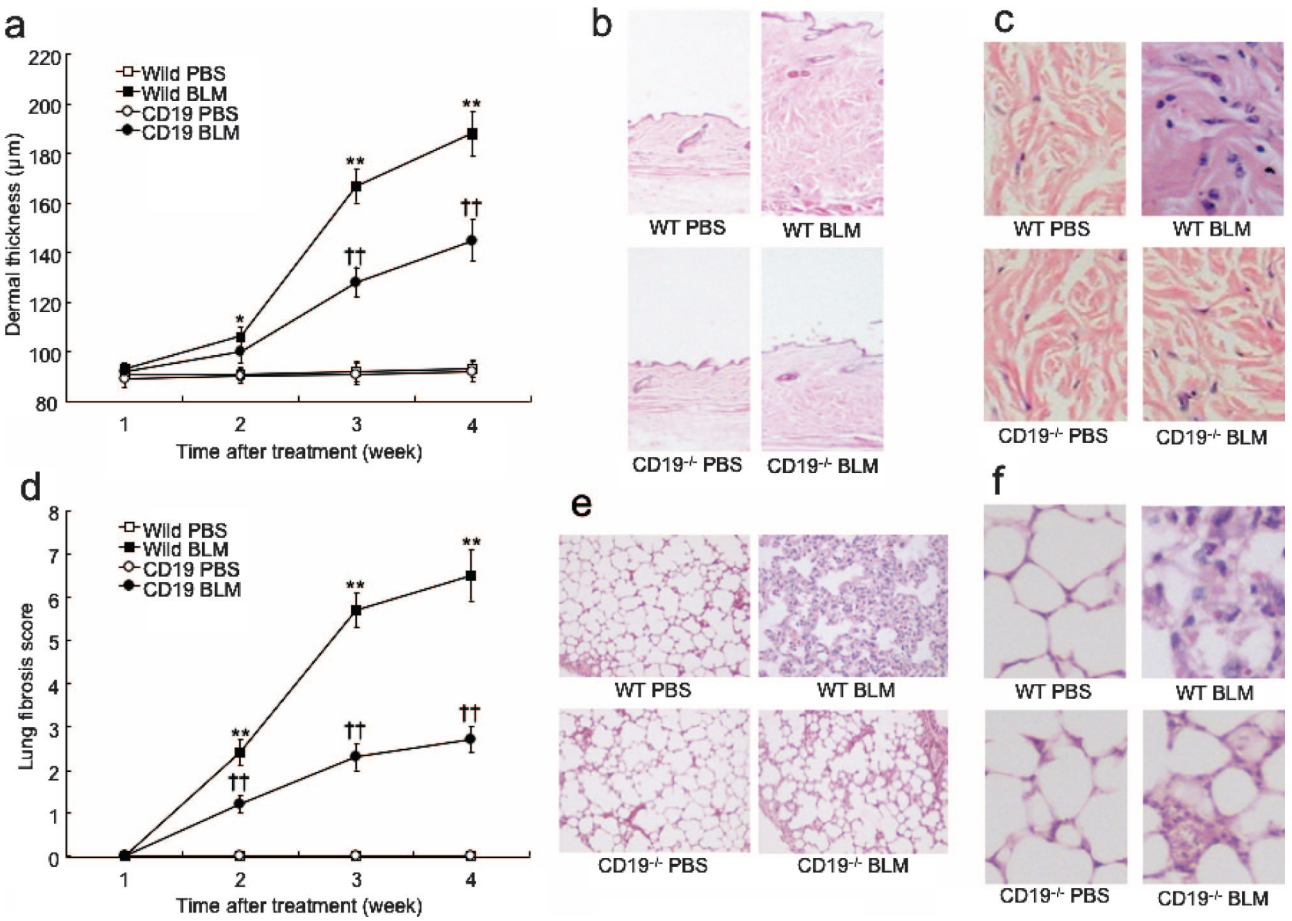

Figure 1. Skin (**a–c**) and lung (**d–f**) fibrosis from WT and CD19$^{-/-}$ mice treated with either BLM or PBS. Skin and lung fibrosis was assessed by quantitatively measuring dermal thickness (**a**) and lung fibrosis score (**d**) 1, 2, 3, and 4 weeks after BLM treatment. Representative histological sections stained with H&E are shown. These results represent those obtained with at least 10 mice of each group. The dermal thickness and lung fibrosis score were measured under a light microscope. Each histogram shows the mean (±SD) results obtained for 10 mice of each group. $^{*}P < 0.05$, $^{**}P < 0.005$ versus PBS-treated mice and $^{\dagger\dagger}P < 0.005$ versus BLM-treated WT mice. Original magnifications: ×40 (**b**, **e**); ×200 (**c**, **f**).

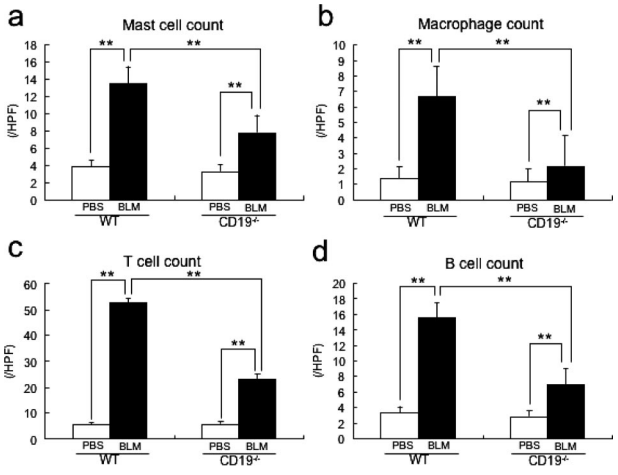

Figure 2. The number of mast cells (**a**), macrophages (**b**), T cells (**c**), and B cells (**d**) at the BLM-injected site of skin from PBS- or BLM-treated WT and CD19$^{-/-}$ mice. Mast cells were identified by toluidine blue staining, whereas macrophages, T cells, and B cells were stained with F4/80, anti-CD3 mAb, and anti-B220 mAb, respectively. Cells were counted in 10 random grids under magnification of ×400 high-power fields (HPF). Each histogram shows the mean (±SD) results obtained for 10 mice of each group. $^{**}P < 0.005$.

BLM-treated CD 19$^{-/-}$ mice, because previous studies revealed that MIP-2, which is secreted by B cells as well as by macrophages and mast cells, functions as a chemoattractant for macrophages, mast cells, T cells, and neutrophils.[33–39] Therefore, the production of these cytokines in the serum (Figure 3a) and sclerotic skin (Figure 3b) by BLM injection was assessed. BLM-treated WT mice had elevated serum levels of IL-4, IL-6, IL-10, IFN-γ, TNF-α, TGF-β1, and MIP-2 compared with PBS-treated WT mice ($P < 0.005$). Serum levels of all cytokines examined in this study were reduced in BLM-treated CD19$^{-/-}$ mice relative to BLM-treated WT mice ($P < 0.005$), but remained elevated compared with PBS-treated CD19$^{-/-}$ mice ($P < 0.05$).

Like serum cytokine levels, mRNA expression levels of IL-4, IL-6, IL-10, IFN-γ, TNF-α, TGF-β1, and MIP-2 in the fibrotic skin from BLM-treated WT mice were higher than those of PBS-treated WT mice ($P < 0.005$). CD19 deficiency inhibited mRNA levels of all examined cytokines, except for IL-10, relative to BLM-treated WT mice ($P < 0.05$). However, mRNA levels of all examined cytokines in the fibrotic skin from BLM-treated CD19$^{-/-}$ mice were still elevated relative to those of PBS-treated CD19$^{-/-}$ mice ($P < 0.05$). Thus, in the serum and sclerotic

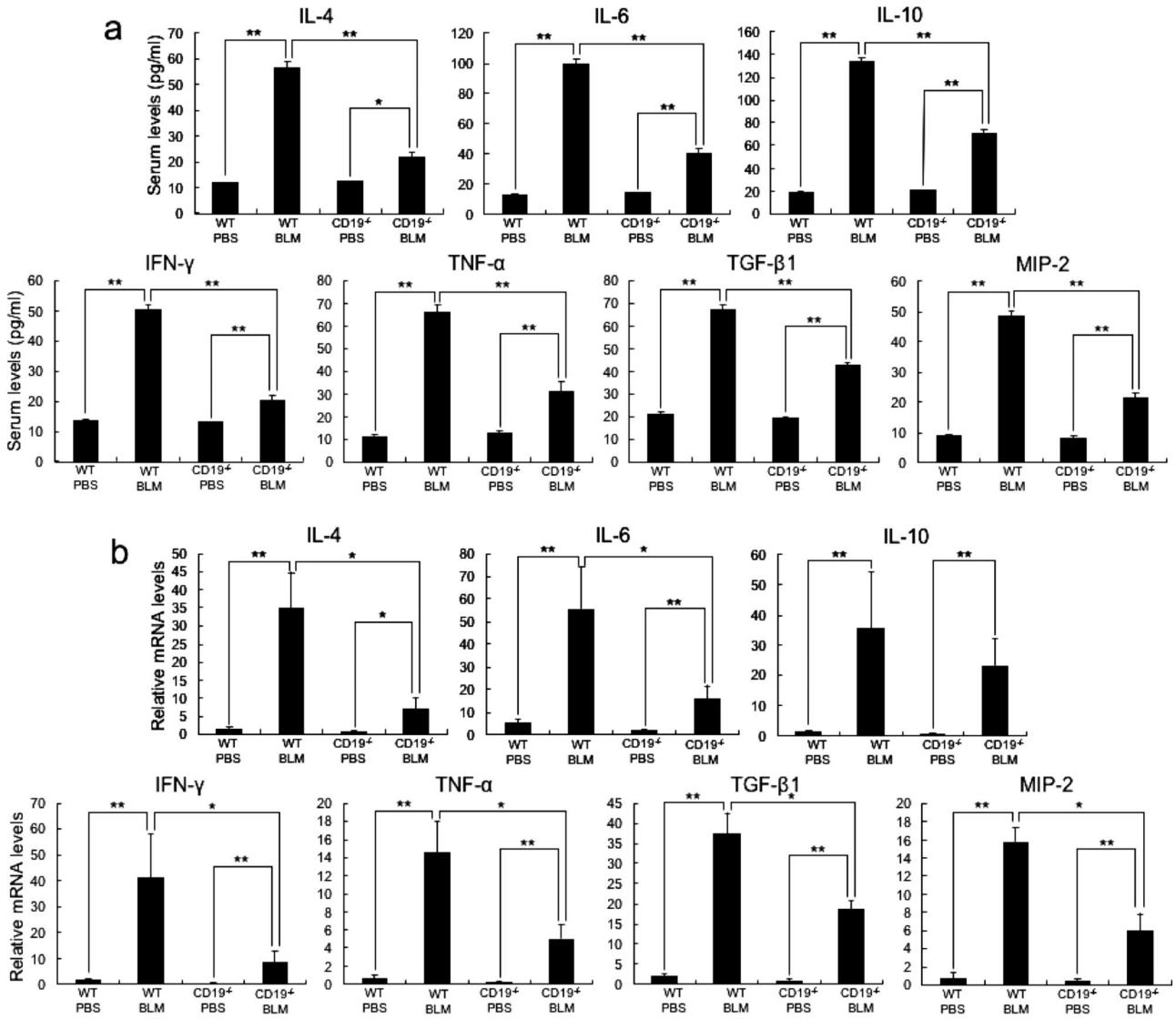

Figure 3. Levels of IL-4, IL-6, IL-10, IFN-γ, TNF-α, TGF-β1, and MIP-2 in serum samples (**a**) and their mRNA expression in the skin (**b**) from WT and CD19$^{-/-}$ mice treated with either PBS or BLM. Serum cytokine levels were assessed using specific ELISA. Total RNA was isolated from lower back skin and mRNA expression was analyzed using real-time PCR. Each histogram shows the mean (±SD) results obtained for six mice of each group. $^{*}P < 0.05$, $^{**}P < 0.005$.

skin, BLM treatment induced the expression of various cytokines, which was generally suppressed by CD19 deficiency.

CD19 Deficiency Inhibited Hyaluronan-, Heparan Sulfate-, and HMBG-1-Induced Cytokine Overproduction by B Cells

Recent studies have shown that breakdown products of the extracellular matrix (ECM), such as hyaluronan and heparan sulfate, stimulate TLR as endogenous ligands for TLR and regulate inflammatory responses.[40,41] Indeed, hyaluronan fragments, which are generated after tissue injury and inflammation, stimulate macrophage chemokine production in a TLR4- and TLR2-dependent manner.[42] Moreover, HMBG-1 released from apoptotic or damaged cells induces acute inflammatory responses through TLR2 and TLR4.[43] Therefore, we investigated whether or not ECMs, such as hyaluronan, heparan sulfate, and chondroitin sulfate, and HMBG-1 could stimulate B cells. The background mRNA and protein levels of all examined cytokines were similar between WT and CD19$^{-/-}$ splenic B cells (Figure 4, a and b). Stimulation of WT B cells with a combination of high- and low-molecular weight hyaluronan (50 to 8000 kDa) increased mRNA and protein levels of IL-4, IL-6, IL-10, IFN-γ, TNF-α, TGF-β1, and MIP-2 compared to media alone ($P < 0.05$). CD19 deficiency suppressed mRNA and protein levels of all examined cytokines, except for TNF-α, by hyaluronan-treated WT B cells ($P < 0.05$), but not to background levels. When compared with backgrounds, WT B cells stimulated with heparan sulfate had elevated mRNA and protein expression of IL-6, IL-10, IFN-γ, TNF-α, and MIP-2 ($P < 0.05$); CD19 deficiency inhibited the expression of all of these except TNF-α ($P < 0.05$). The stimulation of

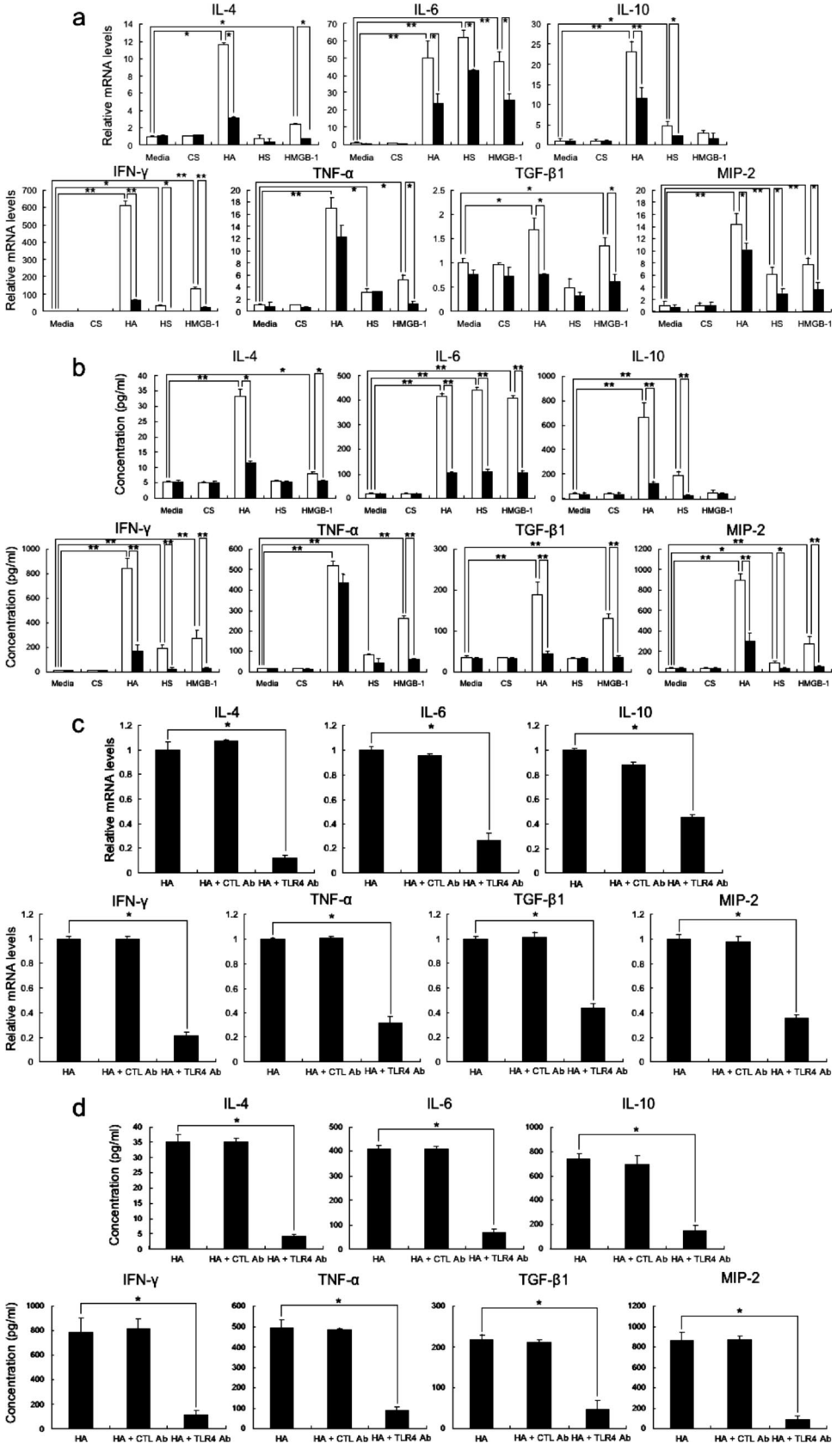
a
IL-4
IL-6
IL-10
IFN-γ
TNF-α
TGF-β1
MIP-2
Relative mRNA levels
Media
CS
HA
HS
HMGB-1
b
Concentration (pg/ml)
c
HA
HA + CTL Ab
HA + TLR4 Ab
d

WT B cells with HMGB-1 also increased mRNA and protein levels of all examined cytokines that CD19 deficiency suppressed, except for IL-10 ($P < 0.05$). Although the effects of heparan sulfate and of HMGB-1 were generally modest relative to that of hyaluronan, the effect by HMGB-1 on IL-6 and TGF-β1 and the effect by heparan sulfate on IL-6 were similar to those by hyaluronan. In contrast, stimulation with chondroitin sulfate did not affect cytokine expression.

We then assessed whether or not anti-TLR4 mAb inhibited hyaluronan-induced B-cell cytokine production (Figure 4, c and d). WT B cells treated with hyaluronan and anti-TLR4 mAb inhibited mRNA expression and protein production of IL-4, IL-6, IL-10, IFN-γ, TNF-α, TGF-β1, and MIP-2 compared with WT B cells treated with hyaluronan alone (56 to 87% decrease, $P < 0.05$). In contrast, control Ab did not affect cytokine production. Thus, ECM, especially hyaluronan, and HMGB-1 stimulated B cells to produce various cytokines, mainly through TLR4, in a CD19-dependent manner.

Low-Molecular Weight Hyaluronan Induced Fibrogenic Cytokine Production by B Cells Mainly through TLR4

Hyaluronan's biological functions differ depending on its molecular weight[44,45]: at high-molecular weight, hyaluronan protects against acute lung injury,[42] whereas at low-molecular weight it has a strong inflammatory function.[45] Therefore, we investigated whether or not low-molecular weight hyaluronan also activates B cells and induces fibrogenic cytokines, such as IL-4, IL-6, and TGF-β1, through TLR4. Stimulation of B cells with low-molecular weight hyaluronan (15 to 40 kDa) increased production of fibrogenic IL-4, IL-6, and TGF-β1 compared to media alone ($P < 0.05$, Figure 5). B cells treated with low-molecular weight hyaluronan and anti-TLR4 mAb inhibited production of these cytokines compared with WT B cells treated with low-molecular weight hyaluronan alone (81 to 84% decrease, $P < 0.05$; Figure 5). Control Ab did not affect production of these cytokines (data not shown). Thus, low-molecular weight hyaluronan also stimulated B cells to produce fibrogenic cytokines, such as IL-4, IL-6, and TGF-β1, mainly through TLR4.

CD19 Deficiency Suppressed BLM-Induced Hyaluronan Overproduction

Hyaluronan expression was only faintly detected in the dermis and lung interstitium from PBS-treated WT mice (Figure 6, a and b). Remarkably, BLM treatment induced hyaluronan expression in dermal fibroblasts, dermal collagen bundles, alveolar epithelium, and alveolar interstitium compared with PBS-treated WT mice. In BLM-treated CD19$^{-/-}$ mice, hyaluronan was also diffusely found in the dermis and lung interstitium; however, the staining intensity was markedly reduced relative to that in BLM-treated WT mice. Serum hyaluronan levels were also assessed (Figure 6c). BLM-treated WT mice had higher serum hyaluronan levels than PBS-treated WT mice ($P < 0.005$). In contrast, BLM-treated CD19$^{-/-}$ mice had decreased hyaluronan levels compared with BLM-treated WT mice ($P < 0.005$), but remained higher than PBS-treated CD19$^{-/-}$ mice ($P < 0.005$). Thus, the loss of CD19 expression inhibited BLM's enhancement of hyaluronan production.

BLM Increased Cytokine Production by LPS-Stimulated B Cells

It has been demonstrated that BLM induces several cytokines by various cell types, such as macrophages, dendritic cells, and lung epithelial cells.[18,19,30–32,42] Therefore, we assessed the responsiveness of WT and CD19$^{-/-}$ B cells stimulated with LPS, an exogenous ligand for TLR4, to various concentrations of BLM. In the absence of BLM, the production of all examined cytokines by LPS-stimulated CD19$^{-/-}$ B cells was lower than that of LPS-stimulated WT B cells. Treatment with 50 ng/ml of BLM most strongly induced production of all examined cytokines by LPS-stimulated WT and CD19$^{-/-}$ B cells ($P < 0.05$, Figure 7). CD19 deficiency reduced BLM-induced production of all examined cytokines at least one BLM concentration ($P < 0.05$). However, cytokine production by CD19$^{-/-}$ B cells treated with 50 ng/ml of BLM was still higher than that of CD19$^{-/-}$ B cells without BLM treatment ($P < 0.05$). Thus, BLM increased the cytokine production by LPS-stimulated B cells, which CD19 deficiency suppressed.

CD19 Loss Reduced Serum Ig Levels in BLM-Treated Mice

The effects of BLM treatment and CD19 loss on B-cell responsiveness were assessed by determining serum Ig levels (Figure 8). PBS-treated CD19$^{-/-}$ mice had lower IgG1, IgG3, and IgA levels compared with PBS-treated WT mice ($P < 0.05$), whereas the levels of other isotypes were similar between these two groups. BLM administration increased serum IgM, IgG1, IgG2a, IgG3, and IgA levels compared with PBS-treated WT mice ($P < 0.05$), whereas it did not affect IgG2b levels. In contrast, BLM-treated CD19$^{-/-}$ mice had decreased IgM, IgG1, IgG2a, IgG2b, IgG3, and IgA levels compared with BLM-treated WT mice ($P < 0.05$). Thus, treatment with BLM induced

Figure 4. Cytokine mRNA expression (**a**) and protein production (**b**) by WT (white bar) and CD19$^{-/-}$ (black bar) B cells stimulated with chondroitin sulfate (CS), hyaluronan (HA), heparan sulfate (HS), or HMGB-1. Purified splenic B cells from WT and CD19$^{-/-}$ mice were stimulated with either media alone, CS, HA, HS, or HMGB-1 for 10 hours. Inhibition of HA-induced cytokine mRNA expression (**c**) and protein production by anti-TLR4 mAb (**d**). Purified splenic B cells from WT and CD19$^{-/-}$ mice were treated with HA and either of anti-TLR4 mAb or control (CTL) Ab. Levels of mRNA expression of IL-4, IL-6, IL-10, IFN-γ, TNF-α, TGF-β1, and MIP-2 were analyzed using real-time PCR. Concentration of these cytokines was analyzed using specific ELISA. Each histogram shows the mean ($\pm$SD) results obtained for six mice of each group. $^{*}P < 0.05$, $^{**}P < 0.005$.

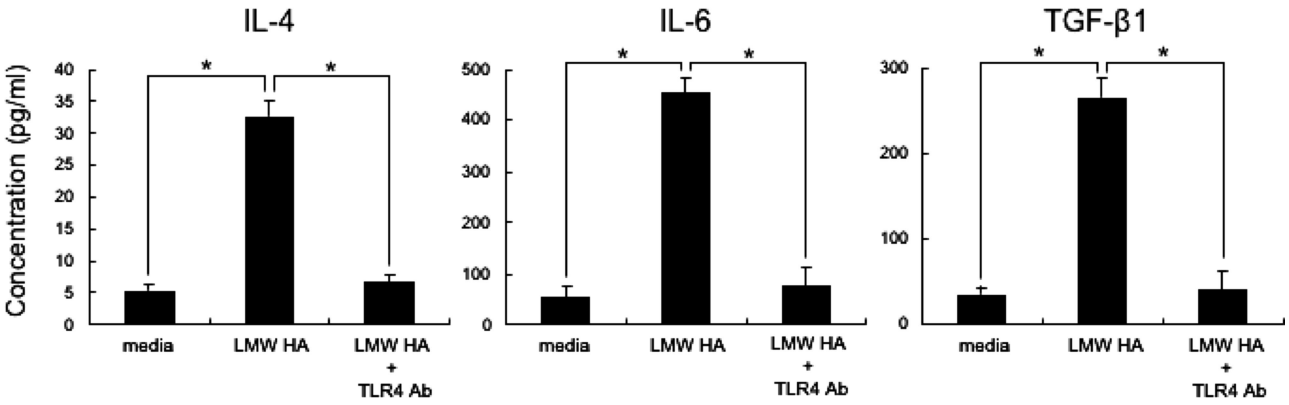

Figure 5. Cytokine production by WT B cells stimulated with low-molecular weight (LMW) HA, and inhibition of LMW HA-induced cytokine production by anti-TLR4 mAb. Purified splenic B cells from WT mice were stimulated with LMW HA in the absence or presence of anti-TLR4 mAb for 10 hours. Concentrations of IL-4, IL-6, and TGF-β1 were analyzed using specific ELISA. Each histogram shows the mean (±SD) results obtained for six mice of each group. *$P < 0.05$.

hyper-γ-globulinemia, which the loss of CD19 expression abrogated.

CD19 Loss Abrogated Autoantibody Production in BLM-Treated Mice

Antinuclear Abs were rarely detectable in PBS-treated WT and CD19$^{-/-}$ mice (6%, 1 of 16, respectively). Antinuclear Abs with a homogenous chromosomal staining pattern were detected in 45% (14 of 31) of BLM-treated WT mice but in only 6% (2 of 31) of BLM-treated CD19$^{-/-}$ mice. Autoantibody specificities were further assessed by ELISA (Figure 9). The dilution of sera giving half-maximal OD values in ELISAs generated arbitrary units per ml that could be directly compared between groups (values in parentheses in Figure 9). PBS-treated CD19$^{-/-}$ mice had decreased IgM autoantibody levels to topo I, U1-RNP, and dsDNA and reduced IgG autoantibody levels to U1-RNP, histones, ssDNA, and dsDNA relative to PBS-treated WT mice ($P < 0.05$). BLM administration in WT mice increased IgG autoantibody production, especially SSc-specific anti-topo I Ab (by 15.7-fold) and anti-histone Ab (by 4.0-fold), as well as IgM autoantibody production (by 1.5- to 2.6-fold), including anti-topo I, anti-U1-RNP, anti-histone, and anti-ssDNA Abs and rheumatoid factor, relative to PBS-treated WT mice ($P < 0.05$). Remarkably, the loss of CD19 expression reduced levels of BLM-induced IgM and IgG Ab to all autoantigens examined in this study to a level similar to that of PBS-treated WT mice. Thus, BLM treatment induced the production of various autoantibodies, especially SSc-specific anti-topo I Ab, that CD19 deficiency eliminated.

Discussion

Transmembrane signals generated through CD19 critically regulate B-cell activation, differentiation, tolerance, and cytokine production by amplifying signals generated through various other receptors.[7,46] The present study is the first to demonstrate that CD19 deficiency inhibited the development of skin and lung fibrosis, hyper-γ-globulinemia, and autoantibody production in a BLM-induced SSc model (Figures 1, 8, and 9), which shares many characteristics of human SSc. Furthermore, CD19 deficiency suppressed the serum and skin production of various cytokines, including fibrogenic IL-4, IL-6, and TGF-β1, that BLM administration induced (Figure 3). Collectively, these results indicate that CD19 expression regulates fibrosis by controlling B-cell production of cytokine in the BLM-induced SSc model.

The reduced dermal fibrosis by CD19 deficiency was associated with the decreased dermal infiltration of macrophages, mast cells, T cells, and B cells (Figure 2), which also infiltrate the fibrotic skin of human SSc patients.[5,25,28,29] This suggests that B-cell activation contributes to downstream inflammatory infiltration of other immune cells. It has been shown that mast cells are attracted by TGF-β1, whereas macrophages are recruited by TGF-β1, IL-6, IL-10, and TNF-α.[38,39,47,48] In the present study, all these cytokines were produced by WT B cells stimulated with hyaluronan (Figure 4). Furthermore, CD19 deficiency inhibited the production of these cytokines except TNF-α (Figure 4). Therefore, the reduced production of these cytokines may partly explain why the loss of CD19 expression suppressed mast cell and macrophage infiltration. Alternatively, because MIP-2, which B cells secrete, can recruit macrophages, mast cells, T cells, and neutrophils,[33–39] the reduced production of MIP-2 by CD19$^{-/-}$ B cells (Figure 4), which is also reflected by the decrease in MIP-2 expression in the serum and fibrotic skin of CD19$^{-/-}$ mice (Figure 3), may in part explain why CD19 deficiency attenuated the migration of macrophages, mast cells, and T cells to sclerotic skin.

TLRs and their ligands contribute to inflammatory responses, including autoimmune diseases, as well as host defenses by innate immunity.[49] Indeed, numerous studies have documented the ability of microbial TLR ligands to trigger disease onset in experimental models of arthritis, experimental allergic encephalomyelitis, myocarditis, diabetes, and atherosclerosis.[50] LPS, a major Gram-negative bacterial component, is an exogenous ligand for TLR4 that induces B-cell activation. Recently, many studies have identified various endogenous ligands for TLR4, such as hyaluronan (especially at low molecular weight),

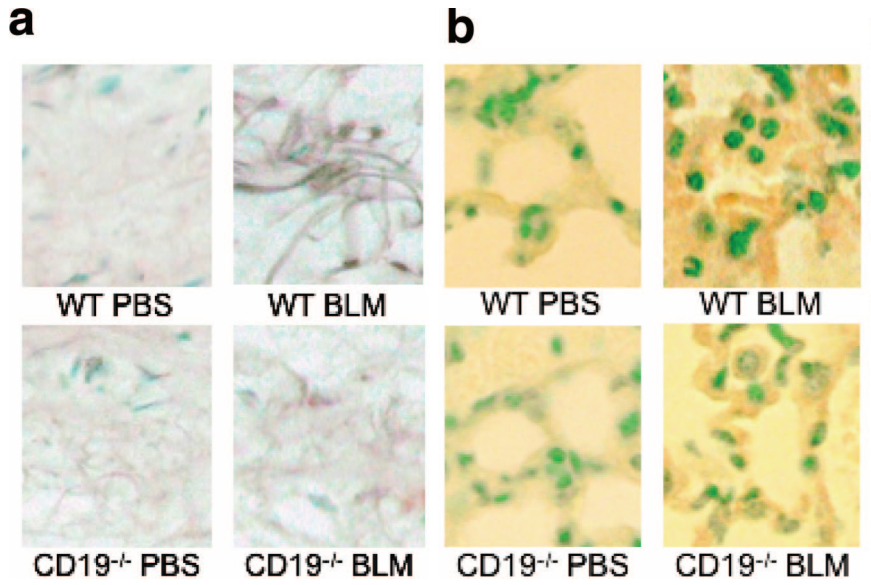

Figure 6. Hyaluronan expression in the skin (**a**), lung (**b**), and serum (**c**) from PBS- or BLM-treated WT and CD19$^{-/-}$ mice. Hyaluronan was stained by biotinylated hyaluronic acid binding protein. The amount of hyaluronan in the serum was quantified using specific ELISA. Histogram shows the mean (±SD) results obtained for six mice of each group. $^{**}P < 0.005$. Original magnifications, ×200.

heparan sulfate, fibrinogen, fibronectin, and HMGB-1, that regulate inflammatory responses.[44,45,50,51] In this study, BLM treatment enhanced hyaluronan production in the skin, lung, and sera (Figure 6). Furthermore, hyaluronan that contained both high- and low-molecular weight hyaluronan, as well as low-molecular weight hyaluronan alone, stimulated B cells to produce various cytokines, mainly via TLR4, whereas heparan sulfate and HMGB-1 had lesser effects (Figures 4 and 5). However, stimulation with heparan sulfate and HMGB-1 induced the production of fibrogenic cytokines, especially IL-6 and TGF-β1, to levels similar to those with hyaluronan, suggesting that heparan sulfate and HMGB-1 also contribute to the development of fibrosis. Remarkably, CD19 deficiency generally inhibited hyaluronan-, heparan sulfate-, and HMGB-1-induced cytokine production by B cells (Figure 4). These results suggest that ECM, especially hyaluronan, and HMGB-1 cooperatively regulate fibrosis by inducing cytokine production by B cells, which is primarily dependent on CD19 signaling. Treatment with anti-TLR4 mAb did not completely suppress cytokine production by B cells stimulated with hyaluronan (Figure 4, c and d; and Figure 5). A recent study has shown that hyaluronan stimulates macrophage chemokine production in a TLR4- and TLR2-dependent manner.[43] Murine B cells express both TLR2 and TLR4.[52] Therefore, the residual cytokine production after TLR4 blockade may be attributable to TLR2 activation by hyaluronan.

Recent studies have revealed an important role of endogenous ligands for TLR2/TLR4 in the development

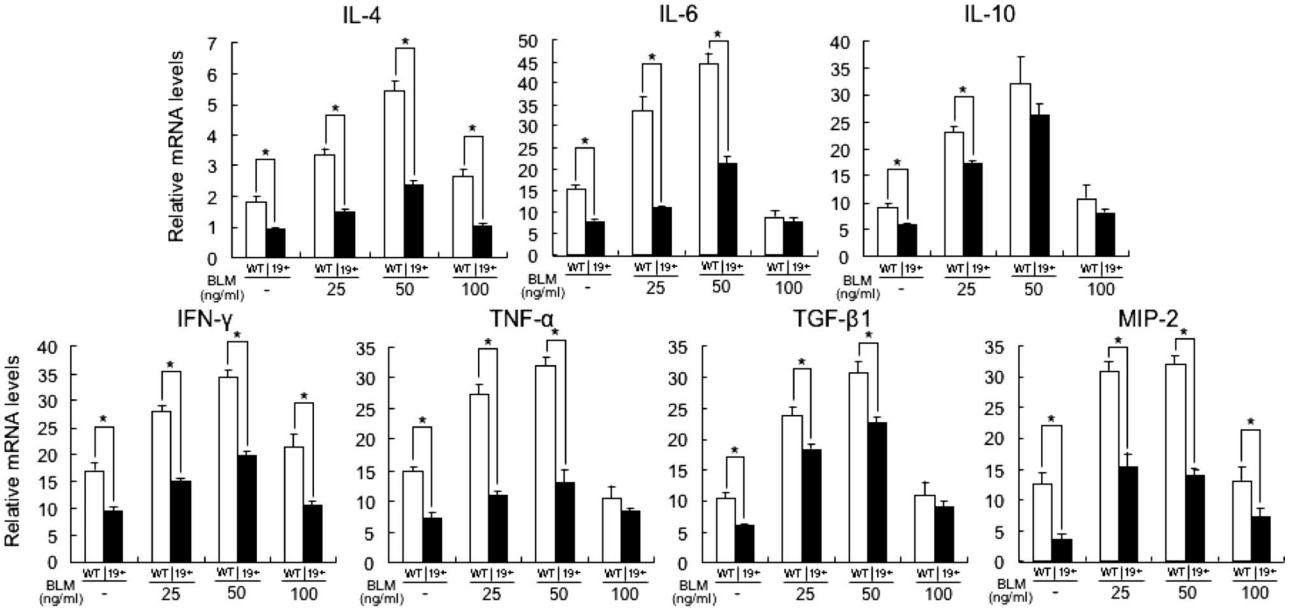

Figure 7. The effect of BLM on cytokine production by WT and CD19$^{-/-}$ (19$^{-/-}$) B cells stimulated with LPS. Purified splenic B cells were stimulated with 25, 50, or 100 ng/ml of BLM in the presence of LPS (1 μg/ml) for 10 hours. Expression of IL-4, IL-6, IL-10, IFN-γ, TNF-α, TGF-β1, and MIP-2 mRNA was analyzed using real-time PCR. Each histogram shows the mean (±SD) results obtained for six mice of each group. $^{*}P < 0.05$.

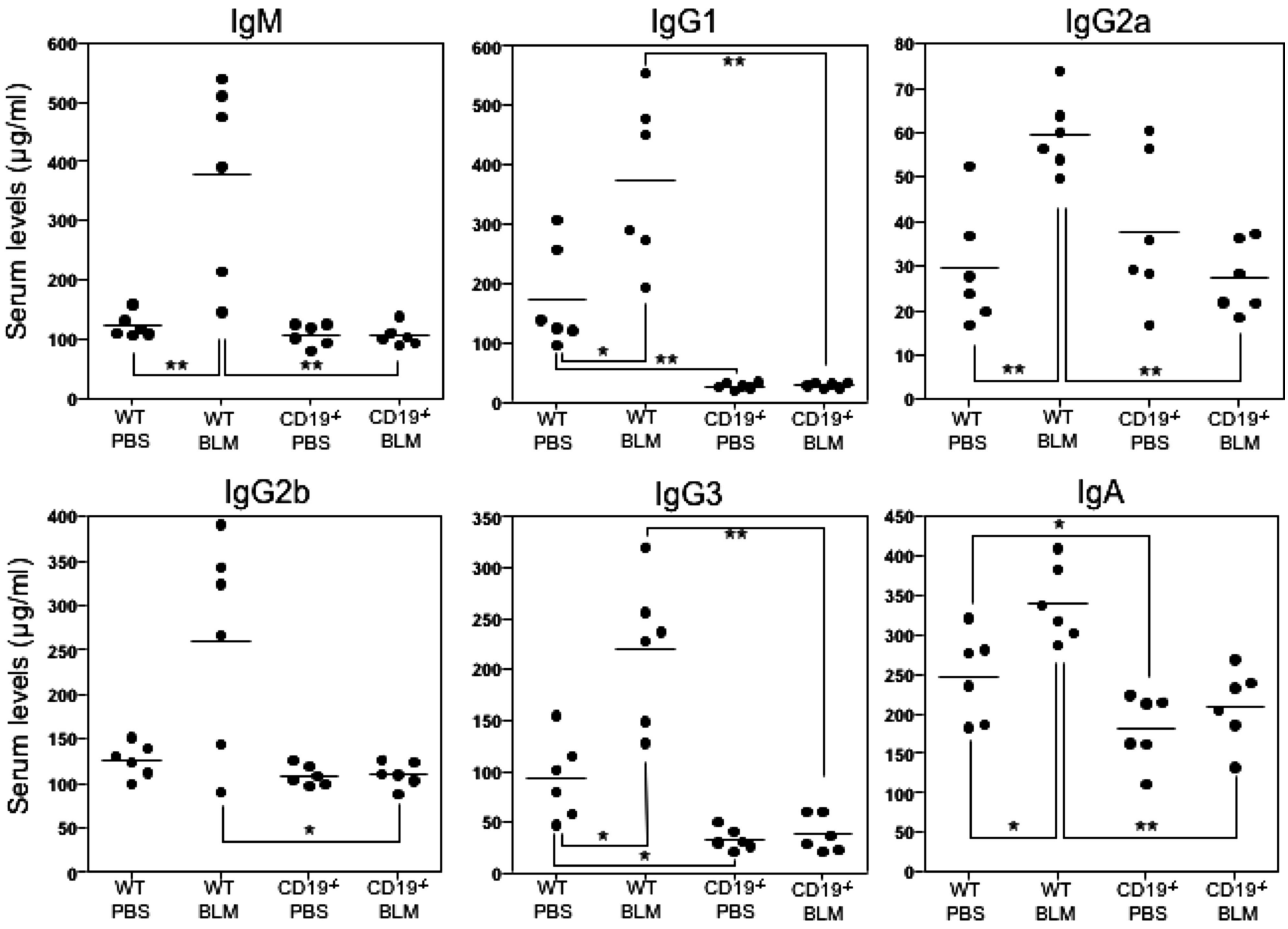

Figure 8. Serum Ig levels in PBS- or BLM-treated WT and CD19$^{-/-}$ mice. Serum samples were obtained by a cardiac puncture 4 weeks after treatment with either BLM or PBS. Serum Ig levels were determined by isotype-specific ELISAs. Horizontal bars represent mean Ig levels. $^{*}P < 0.05$, $^{**}P < 0.005$.

of diseases.[50] The transfer of serum of K/BxN mice, a spontaneous rheumatoid arthritis model, to WT mice induces joint swelling that TLR4 deficiency reduces.[53] Furthermore, TLR2-deficient or TLR4-deficient mice exhibit reduced myocardial ischemia-reperfusion injury.[54,55] In a BLM-induced lung fibrosis model, hyaluronan degradation products stimulate macrophages to produce inflammatory mediators.[42] Moreover, BLM itself directly induces chemokine production by lung epithelial cells in a TLR2- and/or TLR4-dependent manner, contributing to acute lung injury.[42] Similarly, in the present study, BLM itself enhanced cytokine production by B cells stimulated with LPS (Figure 7). Taken together, these results suggest that BLM-induced hyaluronan production is an intrinsic signal of disease expression by activating TLR2/TLR4 signaling, which BLM itself further enhances.

Analysis of a cytokine profile in sera from human SSc patients has revealed that fibrogenic Th2 cytokines, including IL-4 and IL-6, as well as TGF-β1, are predominant.[56–58] Furthermore, a shift from a Th2 to a Th1 response correlates with improvement in skin fibrosis in SSc.[56] However, cytokine production in SSc appears to be more complicated: increased production of some Th1 cytokines, such as IL-12, is also demonstrated.[59] The production of IFN-γ, a potent anti-fibrotic cytokine, is generally inhibited in human SSc, although some reports have shown that IFN-γ production by peripheral blood mononuclear cells is increased.[60] In the present study, the production of Th1 as well as Th2 cytokines and that of TGF-β1 were up-regulated in the skin, lung, and serum (Figure 3). This production pattern was similar to that of hyaluronan-stimulated B cells (Figure 4). These results suggest that hyaluronan stimulation of B cells induced complex cytokine production and that the net effect of these cytokines regulates the development of fibrosis. Furthermore, CD19 deficiency suppressed the production of these cytokines by B cells stimulated with endogenous TLR4 ligands as well as LPS, an exogenous ligand (Figures 4 and 7), suggesting that CD19 influences TLR4 signaling. Indeed, a previous study showed that CD19$^{-/-}$ B cells exhibit reduced proliferation in response to LPS stimulation.[8] CD19 also regulates signals through B-cell-specific LPS receptor RP105.[61] Furthermore, CD19$^{-/-}$ B cells showed decreased tyrosine phosphorylation of mitogen-activated protein kinases, which are downstream of TLR4 signaling (unpublished observation). Thus, CD19 regulates TLR4 signaling in B cells and thereby controls TLR4-induced cytokine production that leads to fibrosis.

In the present study, BLM treatment induced the production of autoantibodies, especially SSc-specific anti-

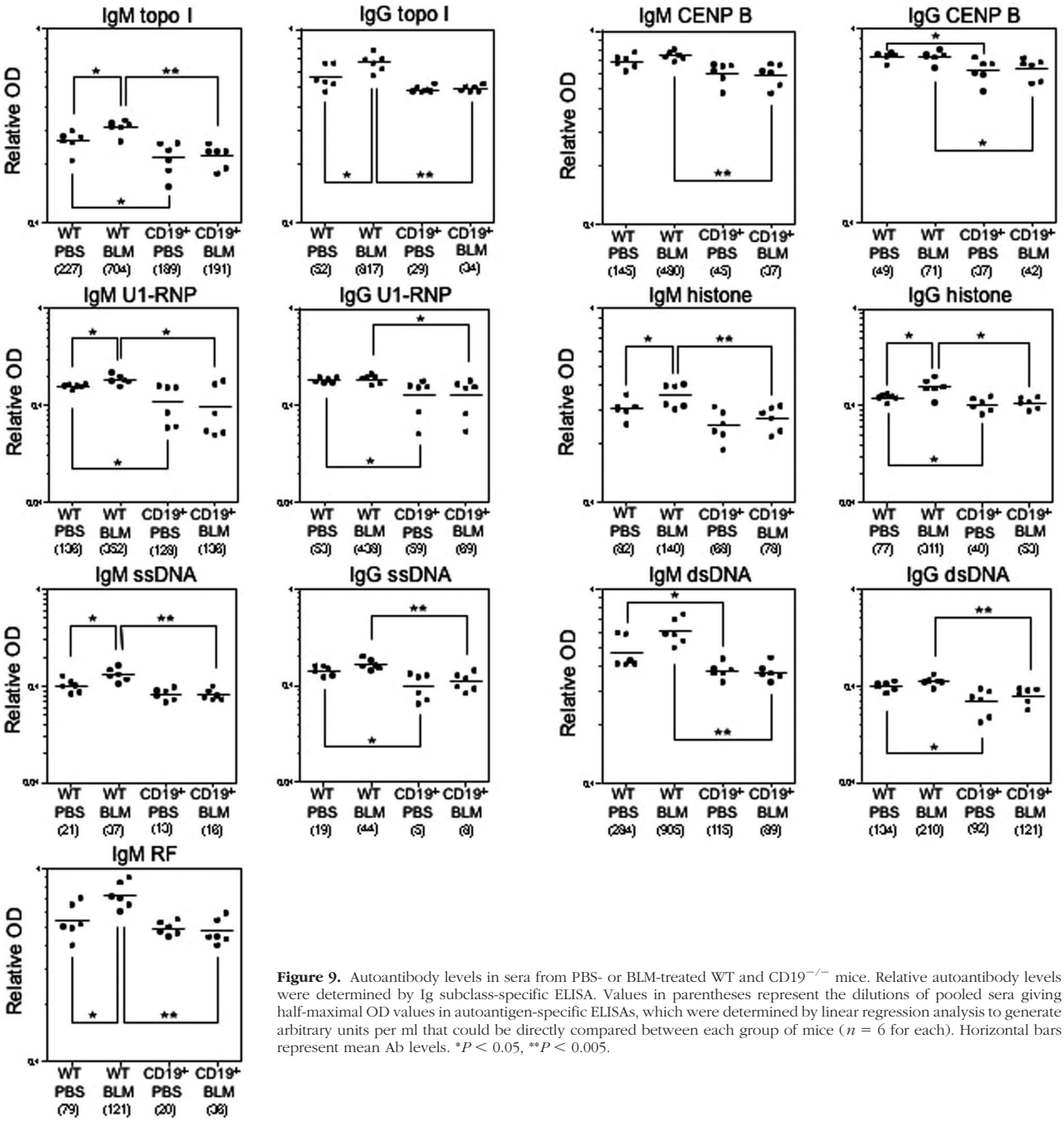

Figure 9. Autoantibody levels in sera from PBS- or BLM-treated WT and CD19$^{-/-}$ mice. Relative autoantibody levels were determined by Ig subclass-specific ELISA. Values in parentheses represent the dilutions of pooled sera giving half-maximal OD values in autoantigen-specific ELISAs, which were determined by linear regression analysis to generate arbitrary units per ml that could be directly compared between each group of mice ($n = 6$ for each). Horizontal bars represent mean Ab levels. $^{*}P < 0.05$, $^{**}P < 0.005$.

topo I Ab, and hyper-γ-globulinemia, both of which are central features of human SSc. It was previously hypothesized that immune responses to autoantigens are induced by cryptic self-epitopes that are generated by the modification of self-antigens during apoptosis.[62] In this regard, topo I is selectively cleaved by Fas (CD95) during apoptosis, and novel cryptic epitopes may be generated.[63] Furthermore, topo I is clustered and concentrated in the surface blebs (apoptotic bodies) of apoptotic cells, which may result in the antigen presentation of cryptic epitopes. In addition, apoptosis is detected in endothelial cells of early inflammatory lesions from patients with SSc.[64] In the BLM-induced SSc model, apoptosis was prominently detected in the skin with up-regulated expression of Fas and FasL.[65] Furthermore, aberrant regulation or expression of TLRs is suggested to predispose an individual to autoantibody production by rendering B cells hyperresponsive to autoantigens.[50] Collectively, BLM-induced apoptosis and hyaluronan-enhanced TLR signaling of B cells may induce autoantibody production. Moreover, the finding that CD19 loss eliminated autoantibody production suggests that CD19 regulates autoantibody production in response to BLM treatment possibly by altering TLR4 signaling.

Acknowledgments

We thank Ms. Yuko Yamada, Masako Matsubara, Aya Usui, Mariko Yozaki, and Kaori Shimoda for technical assistance.

References

1. LeRoy EC, Krieg T, Black C, Medsger TAJ, Fleischmajer R, Rowell N, Jablonska S, Wollheim F: Scleroderma (systemic sclerosis): classification, subsets, and pathogenesis. J Rheumatol 1988, 15:202–205
2. Okano Y: Antinuclear antibody in systemic sclerosis (scleroderma). Rheum Dis Clin North Am 1996, 22:709–735
3. Sato S, Fujimoto M, Hasegawa M, Takehara K: Altered blood B lymphocyte homeostasis in systemic sclerosis: expanded naive B cells and diminished but activated memory B cells. Arthritis Rheum 2004, 50:1918–1927
4. Gudbjornsson B, Hallgren R, Nettelbladt O, Gustafsson R, Mattsson A, af Geijerstam E, Totterman TH: Phenotypic and functional activation of alveolar macrophages. T lymphocytes and NK cells in patients with systemic sclerosis and primary Sjogren's syndrome. Ann Rheum Dis 1994, 53:574–579
5. Kalogerou A, Gelou E, Mountantonakis S, Settas L, Zafiriou E, Sakkas L: Early T cell activation in the skin from patients with systemic sclerosis. Ann Rheum Dis 2005, 64:1233–1235
6. Tashkin DP, Elashoff R, Clements PJ, Goldin J, Roth MD, Furst DE, Arriola E, Silver R, Strange C, Bolster M, Seibold JR, Riley DJ, Hsu VM, Varga J, Schraufnagel DE, Theodore A, Simms R, Wise R, Wigley F, White B, Steen V, Read C, Mayes M, Parsley E, Mubarak K, Connolly MK, Golden J, Olman M, Fessler B, Rothfield N, Metersky M: Cyclophosphamide versus placebo in scleroderma lung disease. N Engl J Med 2006, 354:2655–2666
7. Tedder TF, Poe JC, Fujimoto M, Haas KM, Sato S: The CD19-CD21 signal transduction complex of B lymphocytes regulates the balance between health and autoimmune disease: systemic sclerosis as a model system. Curr Dir Autoimmun 2005, 8:55–90
8. Sato S, Ono N, Steeber DA, Pisetsky DS, Tedder TF: CD19 regulates B lymphocyte signaling thresholds critical for the development of B-1 lineage cells and autoimmunity. J Immunol 1996, 157:4371–4378
9. Inaoki M, Sato S, Weintraub BC, Goodnow CC, Tedder TF: CD19-regulated signaling thresholds control peripheral tolerance and autoantibody production in B lymphocytes. J Exp Med 1997, 186: 1923–1931
10. Sato S, Hasegawa M, Fujimoto M, Tedder TF, Takehara K: Quantitative genetic variation in CD19 expression correlates with autoimmunity. J Immunol 2000, 165:6635–6643
11. Tsuchiya N, Kuroki K, Fujimoto M, Murakami Y, Tedder TF, Tokunaga K, Takehara K, Sato S: Association of a functional CD19 polymorphism with susceptibility to systemic sclerosis. Arthritis Rheum 2004, 50:4002–4007
12. Sato S, Fujimoto M, Hasegawa M, Takehara K, Tedder TF: Altered B lymphocyte function induces systemic autoimmunity in systemic sclerosis. Mol Immunol 2004, 41:1123–1133
13. Matsushita T, Hasegawa M, Yanaba K, Kodera M, Takehara K, Sato S: Elevated serum BAFF levels in patients with systemic sclerosis: enhanced BAFF signaling in systemic sclerosis B lymphocytes. Arthritis Rheum 2006, 54:192–201
14. Saito E, Fujimoto M, Hasegawa M, Komura K, Hamaguchi Y, Kaburagi Y, Nagaoka T, Takehara K, Tedder TF, Sato S: CD19-dependent B lymphocyte signaling thresholds influence skin fibrosis and autoimmunity in the tight-skin mouse. J Clin Invest 2002, 109:1453–1462
15. Matsushita T, Fujimoto M, Hasegawa M, Matsushita Y, Komura K, Ogawa F, Watanabe R, Takehara K, Sato S: BAFF antagonist attenuates the development of skin fibrosis in tight-skin mice. J Invest Dermatol 2007, 127:2772–2780
16. Hasegawa M, Hamaguchi Y, Yanaba K, Bouaziz JD, Uchida J, Fujimoto M, Matsushita T, Matsushita Y, Horikawa M, Komura K, Takehara K, Sato S, Tedder TF: B-lymphocyte depletion reduces skin fibrosis and autoimmunity in the tight-skin mouse model for systemic sclerosis. Am J Pathol 2006, 169:954–966
17. Arnett FC, Cho M, Chatterjee S, Aguilar MB, Reveille JD, Mayes MD: Familial occurrence frequencies and relative risks for systemic sclerosis (scleroderma) in three United States cohorts. Arthritis Rheum 2001, 44:1359–1362
18. Yamamoto T, Takagawa S, Katayama I, Yamazaki K, Hamazaki Y, Shinkai H, Nishioka K: Animal model of sclerotic skin. I: Local injections of bleomycin induce sclerotic skin mimicking scleroderma. J Invest Dermatol 1999, 112:456–462
19. Yamamoto T: The bleomycin-induced scleroderma model: what have we learned for scleroderma pathogenesis? Arch Dermatol Res 2006, 297:333–344
20. Engel P, Zhou L-J, Ord DC, Sato S, Koller B, Tedder TF: Abnormal B lymphocyte development, activation and differentiation in mice that lack or overexpress the CD19 signal transduction molecule. Immunity 1995, 3:39–50
21. Ashcroft T, Simpson JM, Timbrell V: Simple method of estimating severity of pulmonary fibrosis on a numerical scale. J Clin Pathol 1988, 41:467–470
22. Meijerink J, Mandigers C, van de Locht L, Tonnissen E, Goodsaid F, Raemaekers J: A novel method to compensate for different amplification efficiencies between patient DNA samples in quantitative real-time PCR. J Mol Diag 2001, 3:55–61
23. Fujimoto M, Poe JC, Jansen PJ, Sato S, Tedder TF: CD19 amplifies B lymphocyte signal transduction by regulating Src-family protein tyrosine kinase activation. J Immunol 1999, 162:7088–7094
24. Yamamoto T, Takahashi Y, Takagawa S, Katayama I, Nishioka K: Animal model of sclerotic skin. II. Bleomycin induced scleroderma in genetically mast cell deficient WBB6F1-W/W(V) mice. J Rheumatol 1999, 26:2628–2634
25. Yamamoto T, Kuroda M, Nishioka K: Animal model of sclerotic skin. III: Histopathological comparison of bleomycin-induced scleroderma in various mice strains. Arch Dermatol Res 2000, 292:535–541
26. Nakao A, Fujii M, Matsumura R, Kumano K, Saito Y, Miyazono K, Iwamoto I: Transient gene transfer and expression of Smad7 prevents bleomycin-induced lung fibrosis in mice. J Clin Invest 1999, 104:5–11
27. Yaekashiwa M, Nakayama S, Ohnuma K, Sakai T, Abe T, Satoh K, Matsumoto K, Nakamura T, Takahashi T, Nukiwa T: Simultaneous or delayed administration of hepatocyte growth factor equally represses the fibrotic changes in murine lung injury induced by bleomycin. A morphologic study. Am J Respir Crit Care Med 1997, 156:1937–1944
28. Hawkins RA, Claman HN, Clark RA, Steigerwald JC: Increased dermal mast cell populations in progressive systemic sclerosis: a link in chronic fibrosis? Ann Intern Med 1985, 102:182–186
29. Whitfield ML, Finlay DR, Murray JI, Troyanskaya OG, Chi JT, Pergamenschikov A, McCalmont TH, Brown PO, Botstein D, Connolly MK: Systemic and cell type-specific gene expression patterns in scleroderma skin. Proc Natl Acad Sci USA 2003, 100:12319–12324
30. Nakagome K, Dohi M, Okunishi K, Tanaka R, Miyazaki J, Yamamoto K: In vivo IL-10 gene delivery attenuates bleomycin induced pulmonary fibrosis by inhibiting the production and activation of TGF-beta in the lung. Thorax 2006, 61:886–894
31. Smith RE, Strieter RM, Phan SH, Lukacs N, Kunkel SL: TNF and IL-6 mediate MIP-1alpha expression in bleomycin-induced lung injury. J Leukoc Biol 1998, 64:528–536
32. Segel MJ, Izbicki G, Cohen PY, Or R, Christensen TG, Wallach-Dayan SB, Breuer R: Role of interferon-gamma in the evolution of murine bleomycin lung fibrosis. Am J Physiol 2003, 285:L1255–L1262
33. Rottem M, Mekori YA: Mast cells and autoimmunity. Autoimmun Rev 2005, 4:21–27
34. Cavaillon JM: Cytokines and macrophages. Biomed Pharmacother 1994, 48:445–453
35. Hu L, Dixit VD, de Mello-Coelho V, Taub DD: Age-associated alterations in CXCL1 chemokine expression by murine B cells. BMC Immunol 2004, 5:15–29
36. Taub D, Dastych J, Inamura N, Upton J, Kelvin D, Metcalfe D, Oppenheim J: Bone marrow-derived murine mast cells migrate, but do not degranulate, in response to chemokines. J Immunol 1995, 154:2393–2402
37. Lippert U, Artuc M, Grutzkau A, Moller A, Kenderessy-Szabo A, Schadendorf D, Norgauer J, Hartmann K, Schweitzer-Stenner R, Zuberbier T, Henz BM, Kruger-Krasagakes S: Expression and functional activity of the IL-8 receptor type CXCR1 and CXCR2 on human mast cells. J Immunol 1998, 161:2600–2608
38. Kitaura J, Kinoshita T, Matsumoto M, Chung S, Kawakami Y, Leitges M, Wu D, Lowell CA, Kawakami T: IgE- and IgE+Ag-mediated mast

cell migration in an autocrine/paracrine fashion. Blood 2005, 105:3222–3229
39. Ishii Y, Yang H, Sakamoto T, Nomura A, Hasegawa S, Hirata F, Bassett DJ: Rat alveolar macrophage cytokine production and regulation of neutrophil recruitment following acute ozone exposure. Toxicol Appl Pharmacol 1997, 147:214–223
40. Termeer C, Benedix F, Sleeman J, Fieber C, Voith U, Ahrens T, Miyake K, Freudenberg M, Galanos C, Simon JC: Oligosaccharides of hyaluronan activate dendritic cells via Toll-like receptor 4. J Exp Med 2002, 195:99–111
41. Johnson GB, Brunn GJ, Platt JL: Cutting edge: an endogenous pathway to systemic inflammatory response syndrome (SIRS)-like reactions through Toll-like receptor 4. J Immunol 2004, 172:20–24
42. Jiang D, Liang J, Fan J, Yu S, Chen S, Luo Y, Prestwich GD, Mascarenhas MM, Garg HG, Quinn DA, Homer RJ, Goldstein DR, Bucala R, Lee PJ, Medzhitov R, Noble PW: Regulation of lung injury and repair by Toll-like receptors and hyaluronan. Nat Med 2005, 11:1173–1179
43. Park JS, Svetkauskaite D, He Q, Kim JY, Strassheim D, Ishizaka A, Abraham E: Involvement of Toll-like receptors 2 and 4 in cellular activation by high mobility group box 1 protein. J Biol Chem 2004, 279:7370–7377
44. Stern R: Hyaluronan catabolism: a new metabolic pathway. Eur J Cell Biol 2004, 83:317–325
45. Stern R, Asari AA, Sugahara KN: Hyaluronan fragments: an information-rich system. Eur J Cell Biol 2006, 85:699–715
46. Matsushita T, Fujimoto M, Hasegawa M, Komura K, Takehara K, Tedder TF, Sato S: Inhibitory role of CD19 in the progression of experimental autoimmune encephalomyelitis by regulating cytokine response. Am J Pathol 2006, 168:812–821
47. Gruber BL, Marchese MJ, Kew RR: Transforming growth factor-beta 1 mediates mast cell chemotaxis. J Immunol 1994, 152:5860–5867
48. Waldmann H: Immunology: protection and privilege. Nature 2006, 442:987–988
49. Janeway CA Jr, Medzhitov R: Innate immune recognition. Annu Rev Immunol 2002, 20:197–216
50. Marshak-Rothstein A: Toll-like receptors in systemic autoimmune disease. Nat Rev Immunol 2006, 6:823–835
51. Lotze MT, Tracey KJ: High-mobility group box 1 protein (HMGB1): nuclear weapon in the immune arsenal. Nat Rev Immunol 2005, 5:331–342
52. Barr TA, Brown S, Ryan G, Zhao J, Gray D: TLR-mediated stimulation of APC: distinct cytokine responses of B cells and dendritic cells. Eur J Immunol 2007, 37:3040–3053
53. Choe JY, Crain B, Wu SR, Corr M: Interleukin 1 receptor dependence of serum transferred arthritis can be circumvented by Toll-like receptor 4 signaling. J Exp Med 2003, 197:537–542
54. Oyama J, Blais C Jr, Liu X, Pu M, Kobzik L, Kelly RA, Bourcier T: Reduced myocardial ischemia-reperfusion injury in Toll-like receptor 4-deficient mice. Circulation 2004, 109:784–789
55. Shishido T, Nozaki N, Yamaguchi S, Shibata Y, Nitobe J, Miyamoto T, Takahashi H, Arimoto T, Maeda K, Yamakawa M, Takeuchi O, Akira S, Takeishi Y, Kubota I: Toll-like receptor-2 modulates ventricular remodeling after myocardial infarction. Circulation 2003, 108:2905–2910
56. Matsushita T, Hasegawa M, Hamaguchi Y, Takehara K, Sato S: Longitudinal analysis of serum cytokine concentrations in systemic sclerosis: association of interleukin 12 elevation with spontaneous regression of skin sclerosis. J Rheumatol 2006, 33:275–284
57. Hasegawa M, Sato S, Fujimoto M, Ihn H, Kikuchi K, Takehara K: Serum levels of interleukin 6 (IL-6), oncostatin M, soluble IL-6 receptor, and soluble gp130 in patients with systemic sclerosis. J Rheumatol 1998, 25:308–313
58. Hasegawa M, Fujimoto M, Kikuchi K, Takehara K: Elevated serum levels of interleukin 4 (IL-4),. IL-10, and IL-13 in patients with systemic sclerosis. J Rheumatol 1997, 24:328–332
59. Sato S, Hanakawa H, Hasegawa M, Nagaoka T, Hamaguchi Y, Nishijima C, Komatsu K, Hirata A, Takehara K: Levels of interleukin 12, a cytokine of type 1 helper T cells, are elevated in sera from patients with systemic sclerosis. J Rheumatol 2000, 27:2838–2842
60. Valentini G, Baroni A, Esposito K, Naclerio C, Buommino E, Farzati A, Cuomo G, Farzati B: Peripheral blood T lymphocytes from systemic sclerosis patients show both Th1 and Th2 activation. J Clin Immunol 2001, 21:210–217
61. Yazawa N, Fujimoto M, Sato S, Miyake K, Asano N, Nagai Y, Takeuchi O, Takeda K, Okochi H, Akira S, Tedder TF, Tamaki K: CD19 regulates innate immunity by the Toll-like receptor RP105 signaling in B lymphocytes. Blood 2003, 102:1374–1380
62. Rosen A, Casciola-Rosen L: Autoantigens as substrates for apoptotic proteases: implications for the pathogenesis of systemic autoimmune disease. Cell Death Differ 1999, 6:6–12
63. Casiano CA, Martin SJ, Green DR, Tan EM: Selective cleavage of nuclear autoantigens during CD95 (Fas/APO-1)-mediated T cell apoptosis. J Exp Med 1996, 184:765–770
64. Sgonc R, Gruschwitz MS, Dietrich H, Recheis H, Eric Greshwin M, Wick G: Endothelial cell apoptosis is a primary pathogeneic event underlying skin lesions in avian and human scleroderma. J Clin Invest 1996, 98:785–792
65. Yamamoto T, Nishioka K: Possible role of apoptosis in the pathogenesis of bleomycin-induced scleroderma. J Invest Dermatol 2004, 122:44–50